Archives of Agriculture and Environmental Science 10(4): 664-670 (2025)
https://doi.org/10.26832/24566632.2025.1004015

e-ISSN: 2456-6632

This content is available online at AESA

Archives of Agriculture and Environmental Science

Journal homepage: journals.aesacademy.org/index.php/aaes

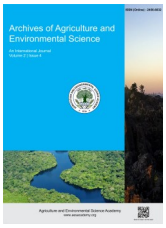

ORIGINAL RESEARCH ARTICLE

Comparing Sentinel-2 vegetation indices for optimal estimation of aboveground carbon stock in a tropical community forest of Nepal

Saroj Kumar Das[1], Ananta Paudel[1], Satish Kumar Singh[2], Sandesh Dhakal[1], Shishu Raj Jha[3] and Yam Bahadur KC[3*]

[1]Institute of Forestry, Tribhuvan University, Pokhara 430469, Nepal
[2]Kathmandu Forestry College, Kathmandu 1276, Nepal
[3]Institute of Forestry, Tribhuvan University, Hetauda 44107, Nepal
[*]Corresponding author's E-mail: yam.kc@hc.tu.edu.np

ARTICLE HISTORY

Received: 08 October 2025
Revised received: 14 December 2025
Accepted: 20 December 2025

Keywords

Aboveground biomass
Carbon stock
Community forest
Red edge
Tropical forest
Vegetation indices

ABSTRACT

Accurate monitoring of forest carbon stocks is essential for effective climate change mitigation. This study aimed to identify the optimal Sentinel-2 vegetation index (VI) for estimating aboveground carbon (AGC) stock in the Raktamala Namuna Community Forest, Nepal. Field data from 53 circular plots (500 m² each) were used to compute AGC based on tree-level dendrometric measurements and species-specific wood density. Ten VIs, including traditional (e.g., NDVI, EVI) and red-edge-based indices (NDVIre1–NDVIre4), were derived from a cloud-free Sentinel-2 Level-2A image (April 7, 2023). Five regression models (linear, logarithmic, quadratic, power, and exponential) were tested for each VI–AGC relationship. The average AGC was 63.88 t·ha^{-1}. The red-edge index NDVIre1 (using Band 5, 705 nm), modelled with a logarithmic function, yielded the highest predictive accuracy (R^2 = 0.7205, r = 0.848, $p < 0.001$), outperforming traditional indices like NDVI (R^2 = 0.609). This study demonstrates the superior sensitivity of Sentinel-2's red-edge band (705 nm) to canopy structure in dense tropical forests. The study concluded that the NDVIre1 logarithmic model provides a novel, cost effective tool for operational and scalable carbon monitoring in community-managed forests, directly supporting REDD+ implementation and localized forest management.

Citation of this article: Das, S. K., Paudel, A., Singh, S. K., Dhakal, S., Jha, S. R., & KC, Y. B. (2025). Comparing Sentinel-2 vegetation indices for optimal estimation of aboveground carbon stock in a tropical community forest of Nepal. *Archives of Agriculture and Environmental Science*, *10*(4), 664-670, https://dx.doi.org/10.26832/24566632.2025.1004015

INTRODUCTION

Forests serve as vital carbon sinks, playing a crucial role in climate change mitigation through photosynthesis. Accurate quantification of forest carbon stocks is therefore fundamental to initiatives like REDD+ (Reducing Emissions from Deforestation and Forest Degradation). Among terrestrial carbon pools, aboveground biomass (AGB) is both dynamic and observable, representing approximately 30% of the total pool, with carbon content estimated as 47% of AGB (IPCC, 2006). While field-based methods provide high-accuracy data, they are often resource-intensive, time-consuming, and challenging to implement across large or inaccessible forest areas. These methods involve rigorous plot establishment, dendrometric measurements, and the application of allometric equations, which, while accurate, limit the spatial extent and frequency of monitoring. In contrast, remote sensing offers a scalable and cost-effective solution for regularly monitoring forest conditions over extensive regions (Ravindranath & Ostwald, 2008; Pandit *et al*., 2018). Among the available remote sensing platforms, Sentinel-2, developed by the European Space Agency (ESA), has emerged as a valuable tool for forest monitoring. It provides high spatial resolution imagery (10–20 meters), frequent revisit intervals (every five days), and enhanced spectral coverage, including red-edge bands that are particularly sensitive to vegetation structure and chlorophyll content (Delegido *et al*., 2011; Gómez, 2017). The red-edge region of the spectrum (approximately 700-750 nm) is where leaf reflectance changes rapidly from low reflectance in

the red (due to chlorophyll absorption) to high reflectance in the near-infrared (due to leaf scattering). This makes it exceptionally useful for assessing vegetation health and density. Various studies have explored the relationship between vegetation indices (VIs) derived from Sentinel-2 imagery and forest biomass, reporting a wide range of correlation strengths, with coefficients of determination (R^2) ranging from 0.017 to 0.54 (Muhe & Argaw, 2022). Despite the growing body of literature, limited research has been conducted in the context of community-managed forests in Nepal, where forest conditions, management practices, and species composition may differ significantly from other regions. Community forests in Nepal are characterized by selective logging, fuelwood collection, and other anthropogenic pressures, which create a heterogeneous forest structure that may challenge broad-spectrum biomass estimation models. Moreover, the potential of Sentinel-2's red-edge bands to overcome this limitation in such managed, complex ecosystems has not been sufficiently explored.

This study addresses this gap by evaluating and comparing the efficacy of traditional and red-edge- based VIs for estimating aboveground carbon (AGC) in a tropical community forest of Nepal. The specific objectives of the study were to estimate AGC using ground-based inventory data; derive a suite of VIs from Sentinel-2 imagery; statistically model the relationship between AGC and each VI and to identify the optimal VI and model for accurate carbon stock estimation in the study area. By combining field measurements with satellite data, this research contributes to the development of scalable, cost effective methodology to enhance carbon monitoring in community managed forests, directly supporting REDD+ implementation and sustainable management practices in Nepal and similar regions.

MATERIALS AND METHODS

Study area

The study was conducted in the Raktamala Namuna Community Forest (RNCF), located in Saptakoshi Municipality, Saptari District, southeastern Nepal (Figure 1). The forest covers 374.42 ha and lies within the tropical bioclimatic zone, with elevations ranging from 371 m to 875 m above sea level and an average slope of 28°. The region experiences a hot summer and a distinct monsoon season, with annual rainfall exceeding 1500 mm. The soil is primarily alluvial and sandy loam. Dominant tree species include *Shorea robusta*, *Anogeissus latifolia*, *Syzygium cumini*, *Mallotus philippinensis*, and *Lagerstroemia parviflora*. To ensure analysis focused exclusively on forested pixels, 48.94 ha of non-forest area (settlements, agriculture) were excluded, leaving 325.47 ha of forested land for analysis.

Field data collection and biomass estimation

A systematic sampling approach was employed using ARcGIS 10.1, at 1% intensity, ensuring uniform spatial coverage and minimizing bias (Gautam *et al.*, 2021). A total of 64 circular plots, each 500 m² (radius = 12.62 m) were initially established. After excluding 11 plots in non-vegetated areas (e.g., rivers and ponds), 53 plots were retained for analysis. Within each plot, all trees with diameter at breast height (DBH) ≥ 5 cm were measured for DBH using a diameter tape and for height using a laser range finder, respectively. Slope corrections were applied to plot boundaries where necessary (Laar & Akça, 2007). Aboveground biomass (AGB) for each tree was calculated using the widely validated pantropical allometric equation (Chave *et al.*, 2005):

$$AGB=0.0509\times\rho x D^2 x H$$

Where:

ρ = wood density (g/cm³), D = diameter at breast height (cm), H = tree height (m).

This equation was selected because it is widely validated for tropical forests and requires only DBH, height, and wood density, making it practical for inventory applications. Wood density values were obtained from species-specific literature or assigned a default value of 0.674 g/cm³ when unavailable (Pandit *et al.*, 2018). Plot level AGB was summed and converted to aboveground carbon (AGC) using the standard IPCC (2006) conversion factor of 0.47. Results were scaled to tons per hectare (t·ha^{-1}).

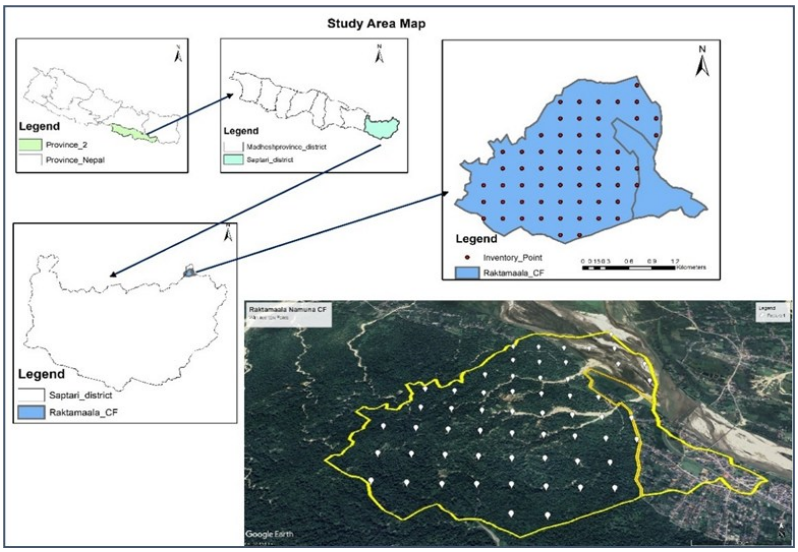

Figure 1. *Location of Raktamala Namuna Community Forest in Saptari District, Nepal.*

Table 1. Sentinel-2 spectral bands used in analysis.

Band Name	Sentinel-2 Band ID
Blue	B2
Green	B3
Red	B4
Red Edge 1	B5
Red Edge 2	B6
Red Edge 3	B7
Near-Infrared (NIR)	B8
Red Edge 4	B8a

Table 2. Vegetation Indices and their formulations

Vegetation Index	Formula	Reference
Normalized Difference Vegetation Index (NDVI)	(NIR – Red)/(NIR + Red)	Rouse *et al.* (1974)
Renormalized Difference Vegetation Index (RDVI)	(NIR – Red)/√(NIR + Red)	Roujean & Breon (1995)
Modified Simple Ratio (MSR)	[(NIR/Red) – 1] / [(NIR/Red)^½ + 1]	Chen (1996)
Ratio Vegetation Index (RVI)	NIR/Red	Pearson & Miller (1972)
Green Normalized Difference Vegetation Index (GNDVI)	(NIR – Green)/(NIR + Green)	Gitelson *et al.* (1996)
Enhanced Vegetation Index (EVI)	2.5 × [(NIR – Red)/(NIR + 6×Red – 7.5×Blue + 1)]	Huete *et al.* (2002)
NDVI re1	(NIR – RE1)/(NIR + RE1)	Gitelson & Merzlyak (1994)
NDVI re2	(NIR – RE2)/(NIR + RE2)	Fernández-Manso *et al.* (2016)
NDVI re3	(NIR – RE3)/(NIR + RE3)	Fernández-Manso *et al.* (2016)
NDVI re4	(NIR – RE4)/(NIR + RE4)	Kross *et al.* (2015)

Satellite image processing and vegetation indices

A cloud free Sentinel-2 Level-2A (Bottom-of-Atmosphere reflectance) image from April 7, 2023, was acquired via the Copernicus Scientific Hub. The image was subset to the study area in ArcMap. Bands B1, B9, B10, B11, and B12 were excluded due to low relevance to vegetation analysis. The remaining spectral bands B2 (Blue, 490 nm), B3 (Green, 560 nm), B4 (Red, 665 nm), B5 (RE1, 705 nm), B6 (RE2, 740 nm), B7 (RE3, 783 nm), B8 (NIR, 842 nm), and B8a (RE4, 865 nm) were used to compute ten vegetation indices (VIs) (Table 1). These indices were selected to represent a range of spectral behaviors, including ratio-based indices (NDVI, RVI), soil-adjusted indices (RDVI), atmospheric-resistant indices (EVI), and indices utilizing the green and red-edge bands, which are known to be sensitive to different vegetation properties. Ten vegetation indices were selected based on their relevance in previous biomass estimation studies. The equations are presented in Table 2.

Pixel value extraction

Using the Zonal Statistics tool in ArcMap, the mean pixel value for each VI was extracted for a circular buffer (radius=12.62 m) around each plot centroid, ensuring spatial correspondence between field and satellite data.

Statistical analysis

Statistical analyses were conducted in RStudio (v4.3.1) and Microsoft Excel. The relationship between plot level AGC ($t \cdot ha^{-1}$) (dependent variable) and each VI (independent variable) was assessed using five regression models:

Linear: $Y = \beta_0 + \beta_1 \times VI$,
Logarithmic: $Y = \beta_0 + \beta_1 \times \ln(VI)$,
Quadratic: $Y = \beta_0 + \beta_1 \times VI + \beta_2 \times VI$,
Power: $Y = \beta_0 \times VI^{\beta_1}$,
Exponential: $Y = \beta_0 \times e^{(\beta_1 \times VI)}$.

Testing the multi-model approach accounts for potential non-linearity and signal saturation in high biomass forests (Kumar & Mutanga, 2017). Model performance was evaluated using the coefficient of determination (R^2) and Pearson's correlation coefficient (r), with statistical significance set at the $p < 0.05$ level. The best-performing model for each VI was selected based on the highest R^2. Models with zero or negative VI values were excluded from fitting power and exponential functions.

RESULTS AND DISCUSSION

Forest composition and carbon stock estimates

During the study, 53 sample plots contained a total of 974 trees from 41 species, indicating relatively high species diversity. *Shorea robusta* was the dominant species, accounting for 61% of the total individuals, followed by *Buchanania latifolia* (7%), *Cascaria graveolens* (4%), *Ehretia acuminata* (3%), and *Semicarpus anacardium* (2%). Descriptive statistics for the measured trees were height (min = 1.5 m, max = 28 m, mean = 10.2 ± 0.16 m) and DBH (min = 5 cm, max = 96 cm, mean = 24.16 ± 0.52 cm). The average aboveground biomass density was 135.91 $t \cdot ha^{-1}$, corresponding to an estimated carbon stock of 63.88 $t \cdot ha^{-1}$. Across the total analyzed forest area of 325. 47 ha, the total aboveground biomass stock was 7,204.17 Mg, with a corresponding carbon stock of 3,385.96 Mg C. The DBH and height distributions indicate a maturing forest with a mix of young and mature trees, characteristic of a managed community forest. Notably, the estimated carbon stock (63.88 $t \cdot ha^{-1}$) is lower than the national average of 82–92 $t \cdot ha^{-1}$ reported by the Forest Resources Assessment/National Forest Inventory (FRA/NFI, 2015). While the national assessment considered trees with DBH ≥ 10 cm and this study included smaller trees (DBH ≥ 5 cm), the contribution of these smaller stems to total biomass is generally modest (5-15%), suggesting that methodological differences alone cannot fully account for the observed

discrepancy. More likely, the reduced carbon stock reflects the forest's status as a community-managed system subject to selective harvesting, fuelwood extraction, and other anthropogenic disturbances that constrain biomass accumulation compared to protected or natural forests typically underpinning national estimates. This interpretation aligns with recent findings by Joshi *et al.* (2020), who reported variable and often lower carbon stocks in Terai community forests due to management impacts. Additionally, the forest's successional stage, dominance by *Shorea robusta*, and local site conditions, such as topography and soil quality, further influence its carbon storage capacity. These findings underscore the necessity of conducting localized, site-specific carbon assessments to ensure accurate carbon accounting and to establish realistic baselines for REDD+ initiatives, rather than relying on generalized national figures.

Relationship between vegetation indices and AGC stock

Regression analysis revealed significant relationships between aboveground carbon stock (AGC) and vegetation indices (VIs) derived from Sentinel-2 imagery, with 8 out of 10 evaluated indices showing statistically significant associations ($p<0.05$). Across 50 tested regression models (10 VIs × 5 model types), the red-edge index NDVIre1 demonstrated the strongest predictive capability. Its logarithmic model achieved the highest correlation ($r = 0.848$, $R^2 = 0.7205$, $p < 0.001$), significantly outperforming all other indices. Among traditional indices, NDVI, RDVI, EVI, and GNDVI showed strong performance under quadratic models, achieving R^2 values between 0.5792 and 0.6093 and correlation coefficients ranging from 0.74 to 0.78. These results align with established literature highlighting their sensitivity to key biophysical parameters: NDVI responds to chlorophyll content and canopy cover (Rouse *et al.*, 1974); RDVI reduces soil background noise (Roujean and Breon, 1995); EVI corrects for atmospheric and canopy background effects (Huete *et al.*, 2002), and GNDVI, leveraging the green band, offers enhanced sensitivity to chlorophyll concentration (Gitelson *et al.*, 1996). The ratio-based indices RVI and MSR showed moderate predictive ability ($R^2 < 0.45$, $r \approx 0.67$), while two red-edge indices (NDVIre3 and NDVIre4) showed no significant correlation with AGC ($p > 0.05$). The complete results are presented in Table 3 (R^2) and Table 4 (r), while the regression equations for the best performing models of each VI are summarized in Table 5. Despite their effectiveness, these traditional indices are prone to saturation in high-biomass settings, where further increases in leaf area or biomass produce diminishing returns in index response, limiting accuracy in dense forests like the study area. In contrast, the superior performance of NDVIre1 stems from its reliance on Sentinel-2's red-edge Band 5 (~705 nm), which captures the steepest portion of the red-edge reflectance curve. With an R^2 of 0.7205 and an r of 0.848, its predictive power substantially exceeds that of the traditional indices. Unlike traditional visible and NIR bands, the red edge region remains sensitive to variations in leaf area index (LAI), chlorophyll content, and canopy structure without rapid saturation (Delegido *et al.*, 2011), enabling more accurate biomass discrimination in dense, multi-layered tropical forests such as the Raktamala Namuna Community Forest (RNCF). Our findings corroborate studies by Khan *et al.* (2020) and Padilla *et al.* (2017), who also found red-edge indices to be more effective than traditional ones in high-biomass environments. Consistent with this pattern, Muhe & Argaw (2022) demonstrated red-edge indices superior to NDVI for biomass estimation in African montane forests, while Poudel *et al.* (2023) also reported similar advantages of Sentinel-2 red-edge data in Nepal's Chure region. The differential performance among the red-edge indices (NDVIre1 > NDVIre2 > NDVIre3 ≈ NDVIre4) further underscores the spectral specificity of carbon estimation. Band 5 (705 nm) captures the steepest slope of the red-edge reflectance curve, maximizing responsiveness to vegetation structure, whereas Bands 6–8a (used in NDVIre3 and NDVIre4) are increasingly affected by water absorption and atmospheric interference, weakening their correlation with biomass (Kross *et al.*, 2015; Fernández-Manso *et al.*, 2016). This confirms that red-edge bands are not functionally equivalent and must be selected with care.

Table 3. Coefficients of determination (R^2) between AGC and vegetation indices.

VIs	Linear	Logarithmic	Quadratic	Power	Exponential
NDVI	0.599	0.5532	0.6093	0.583	0.6064
GNDVI	0.566	0.5374	0.5792	0.563	0.5751
RDVI	0.606	0.5913	0.6067	0.604	0.5971
EVI	0.607	0.5704	0.607	0.594	0.602
MSR	0.44	-	0.4529	-	0.4349
RVI	0.435	0.4399	0.4529	0.448	0.4519
NDVIre1	0.693	0.7205	0.7169	0.708	0.6709
NDVIre2	0.202	0.1694	0.2144	0.176	0.2058
NDVIre3	0.023	-	0.0237	-	0.0224
NDVIre4	0.038	-	0.0399	-	0.0385

Note: Blank cells indicate that the model could not be generated due to zero or negative values of VIs.

Table 4. Correlation coefficients (r) between AGC and vegetation indices.

VIs	Linear	Logarithmic	Quadratic	Power	Exponential
NDVI	0.77***	0.74***	0.78***	0.76***	0.77***
GNDVI	0.752***	0.733***	0.761***	0.75***	0.758***
RDVI	0.778***	0.768***	0.778***	0.777***	0.772***
EVI	0.779***	0.755***	0.779***	0.770***	0.775***
MSR	0.663**	-	0.673**	-	0.659**
RVI	0.663***	0.671***	0.672***	0.669***	0.659***
NDVIre1	0.832***	0.848***	0.846***	0.841***	0.819***
NDVIre2	0.448***	0.411**	0.463***	0.419***	0.453***
NDVIre3	0.155	-	0.154	-	0.149
NDVIre4	0.195	-	0.199	-	0.196

Note: ***p < 0.001, **p < 0.01. Blank cells indicate insufficient data for model calculation.

Table 5. Best-performing Regression Models for each vegetation index.

Vegetation Index	Best Model	Regression Equation	R^2
NDVI	Quadratic	$y = 218.57x^2 + 2.0411x + 54.312$	0.6093
GNDVI	Quadratic	$y = 543.48x^2 - 116.28x + 62.329$	0.5792
RDVI	Quadratic	$y = -0.0121x^2 + 2.4773x + 28.285$	0.6067
EVI	Quadratic	$y = -30.242x^2 + 537.1x + 42.611$	0.607
NDVIre1	Logarithmic	$y = 41.048\ln(x) + 148.22$	0.7205
RVI	Quadratic	$y = -12.506x^2 + 56.451x + 24.823$	0.4529
MSR	Quadratic	$y = -72.893x^2 + 75.898x + 68.767$	0.4529
NDVIre2	Quadratic	$y = 3596.5x^2 - 62.638x + 74.246$	0.2144
NDVIre3	Quadratic	$y = -1457.4x^2 + 155.81x + 79.534$	0.0237
NDVIre4	Quadratic	$y = 2316.9x^2 + 275.86x + 85.137$	0.0399

Note: x represents vegetation index value; y represents aboveground carbon stock ($t \cdot ha^{-1}$).

Spatial mapping of carbon stock

Using the best -performing NDVIre1 logarithmic model, a spatial map of AGC stock was generated for the entire 325.47-ha community forest (Figure 2). The map reveals marked spatial heterogeneity: higher carbon stocks (> 80 $t \cdot ha^{-1}$) are concentrated in the forest interior with dense vegetation, while lower values (< 40 $t \cdot ha^{-1}$) occur near rivers, roads, agricultural margins, and other disturbance prone edges. This pattern aligns with ecological expectations, as forest edges experience higher human activity, microclimate stress, and reduced tree density, all of which limit carbon accumulation. Recent studies, including Gautam *et al.* (2021), have mapped similar spatial carbon variability in Nepalese community forests, directly linking it to management access and disturbance regimes. Beyond accurate estimation, this mapping capability demonstrates the practical utility of the Sentinel-2 NDVIre1 model. It provides forest managers and REDD+ stakeholders with a cost effective, scalable tool not only to quantify total carbon but also to identify spatial patterns of storage and loss, enabling targeted conservation and sustainable forest management interventions. These findings have crucial implications for forest carbon monitoring. They show that Sentinel-2's red-edge band (B5) provides a powerful, practical tool for large-scale, accurate AGC mapping in tropical forests. While traditional indices remain valuable for general vegetation monitoring, NDVIre1 with a logarithmic model emerges as the preferred choice for high-precision carbon assessment in dense, tropical, community-managed forests. This evidence supports the integration of Sentinel-2 data into national REDD+ frameworks and community-based forest management programs, enabling cost effective, scalable, and frequent monitoring that directly contributes to conservation efforts and climate change mitigation strategies.

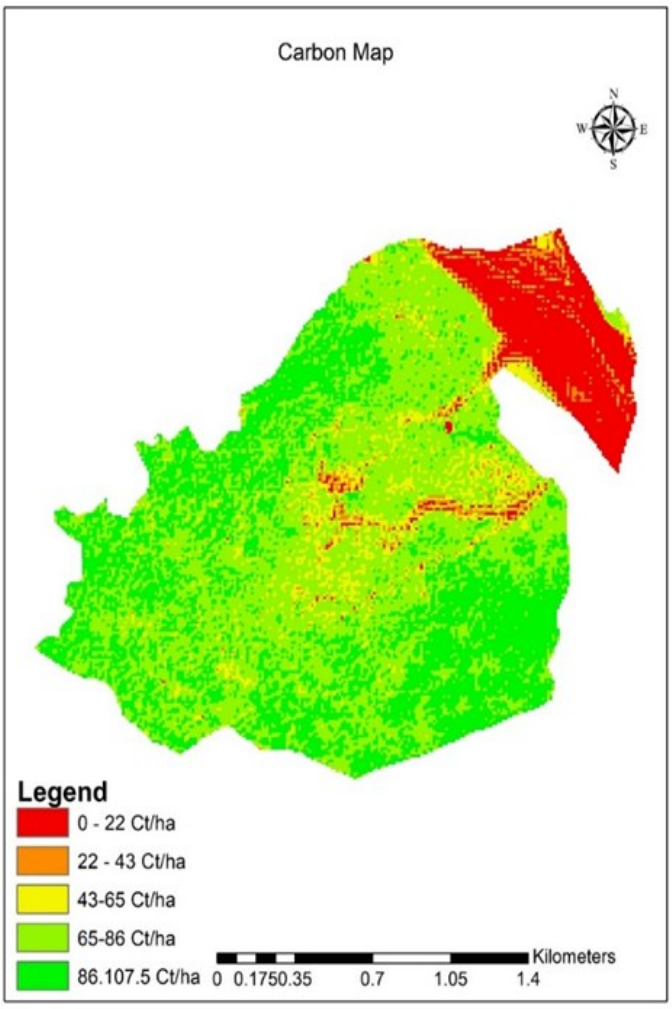

Figure 2. *Predicted aboveground carbon stock (AGC in $t \cdot ha^{-1}$) map of Raktamala Namuna community forest, generated using the logarithmic model of the NDVIre1 index.*

Conclusion

This study demonstrates the efficacy of Sentinel-2 satellite data for estimating aboveground carbon stock (AGC) in tropical community forests of Nepal. The red-edge based vegetation index NDVIre1 modelled using a logarithmic function, provided the strongest predictive capability (r = 0.848, R^2 = 0.7205), significantly outperforming conventional indices such as NDVI. This highlights the superior sensitivity of Sentinel-2's red-edge bands to the complex canopy structures found in managed tropical forests. While traditional VIs (e.g., NDVI, RDVI, EVI, GNDVI) also showed strong correlations, NDVIre1 is recommended as the optimal index for accurate, high-resolution carbon mapping in similar ecological contexts. Future efforts should focus on validating this model across varied ecological and management conditions, developing localized allometric equations, and integrating Sentinel-2 data with LiDAR or other structural sensors for improved precision. Incorporating this methodology into national REDD+ frameworks and community-based forest management programs can enable cost-effective, reliable carbon accounting, supporting both local conservation goals and global climate change mitigation strategies.

ACKNOWLEDGEMENT

We thank Dr. Ramsheshwor Mandal for his guidance throughout this research, Division Forest Office, Saptari, for logistical support, and the Institute of Forestry, Tribhuvan University, (Pokhara Campus and Hetauda Campuses) for their academic support.

DECLARATIONS

Author contribution statement: Conceptualization: S.K.D. and Y.B.K.; Methodology: S.K.D.; Software and validation: A.P., S.K.D. and S.K.S.; Formal analysis and investigation: S.K.D.; Resources: S.R.S.; Data curation: S.D.; Writing—original draft preparation: S.K.D.; Writing—review and editing: Y.B.K.; Visualization: S.D.; Supervision: Y.B.K.; Project administration: S.R.S.; Funding acquisition: S.R.S. All authors have read and agreed to the published version of the manuscript.

Conflicts of interest: The authors declare that there are no conflicts of interest regarding the publication of this manuscript.

Ethics approval: This study did not involve any animal or human participant and thus ethical approval was not applicable.

Consent for publication: All co-authors gave their consent to publish this paper in AAES.

Data availability: The data that support the findings of this study are available on request from the corresponding author.

Supplementary data: No supplementary data is available for the paper.

Funding statement: No external funding is available for this study.

Additional information: No additional information is available for this paper.

REFERENCES

Chave, J., Andalo, C., Brown, S., Cairns, M. A., Chambers, J. Q., Eamus, D., Fölster, H., Fromard, F., Higuchi, N., Kira, T., Lescure, J. P., Nelson, B. W., Ogawa, H., Puig, H., Riéra, B., & Yamakura, T. (2005). Tree allometry and improved estimation of carbon stocks and balance in tropical forests. *Oecologia*, *145*(1), 87–99. https://doi.org/10.1007/s00442-005-0100-x

Chen, J. M. (1996). Evaluation of vegetation indices and a modified simple ratio for boreal applications. *Canadian Journal of Remote Sensing*, *22*(3), 229–242. https://doi.org/10.1080/07038992.1996.10855178

Delegido, J., Verrelst, J., Alonso, L., & Moreno, J. (2011). Evaluation of Sentinel-2 red-edge bands for empirical estimation of green LAI and chlorophyll content. *Sensors*, *11*(7), 7063–7081. https://doi.org/10.3390/s110707063

Fernández-Manso, A., Fernández-Manso, O., & Quintano, C. (2016). SENTINEL-2A red-edge spectral indices suitability for discriminating burn severity. *International Journal of Applied Earth Observation and Geoinformation*, *50*, 170–175. https://doi.org/10.1016/j.jag.2016.03.005

FRA/NFI, Forest Resource Assessment Nepal. (2015). *State of Nepal's forests*. Department of Forest Research and Survey.

Gautam, B., Mandal, R. A., & Badal, D. (2021). *Forest carbon dynamic according to altitudinal gradient in Nepal* [Unpublished report]. Institute of Forestry.

Gitelson, A. A., Kaufman, Y. J., & Merzlyak, M. N. (1996). Use of a green channel in remote sensing of global vegetation from EOS-MODIS. *Remote Sensing of Environment*, *58*(3), 289–298. https://doi.org/10.1016/S0034-4257(96)00072-7

Gitelson, A. A., & Merzlyak, M. N. (1994). Spectral reflectance changes associated with autumn senescence of *Aesculus hippocastanum* L. and *Acer platanoides* L. leaves. Spectral features and relation to chlorophyll estimation. *Journal of Plant Physiology*, *143*(3), 286–292. https://doi.org/10.1016/S0176-1617(11)81633-0

Gómez, M. (2017). Joint use of Sentinel-1 and Sentinel-2 for land cover classification: A machine learning approach [Master's thesis, Lund University]. https://lup.lub.lu.se/student-papers/search/publication/8915043

Huete, A., Didan, K., Miura, T., Rodriguez, E. P., Gao, X., & Ferreira, L. G. (2002). Overview of the radiometric and biophysical performance of the MODIS vegetation indices. *Remote Sensing of Environment*, *83*(1–2), 195–213. https://doi.org/10.1016/S0034-4257(02)00096-2

IPCC, Intergovernmental Panel on Climate Change. (2006). *2006 IPCC guidelines for national greenhouse gas inventories*. Institute for Global Environmental Strategies. https://www.ipcc-nggip.iges.or.jp/public/2006

Joshi, R., Singh, H., Chhetri, R., & Yadav, K. (2020). Assessment of carbon sequestration potential in degraded and non-degraded community forests in Terai region of Nepal. *Journal of Forest and Environmental Science*, *36*(2), 113–121. https://doi.org/10.7747/JFES.2020.36.2.113

Khan, K., Iqbal, J., Ali, A., & Khan, S. N. (2020). Assessment of Sentinel-2-derived vegetation indices for the estimation of above-ground biomass/carbon stock, temporal deforestation and carbon emissions estimation in the moist temperate forests of Pakistan. *Applied Ecology and Environmental Research*, *18*(1), 783–815. https://doi.org/10.15666/aeer/1801_783815

Kross, A., McNairn, H., Lapen, D., Sunohara, M., & Champagne, C. (2015). Assessment of RapidEye vegetation indices for estimation of leaf area index and biomass in corn and soybean crops. *International Journal of Applied Earth Observation and Geoinformation*, *34*, 235–248. https://doi.org/10.1016/j.jag.2014.08.002

Kumar, L., & Mutanga, O. (2017). Remote sensing of above-ground biomass. *Remote Sensing*, *9*(9), 935. https://doi.org/10.3390/rs9090935

Laar, A. V., & Akça, A. (2007). *Forest mensuration* (Vol. 13). Springer. https://doi.org/10.1007/978-1-4020-5991-9

Muhe, S., & Argaw, M. (2022). Estimation of above-ground biomass in tropical afromontane forest using Sentinel-2 derived indices. *Environmental Systems Research*, *11*(1), 5. https://doi.org/10.1186/s40068-022-00250-y

Padilla, F. M., Peña-Fleitas, M. T., Gallardo, M., & Thompson, R. B. (2017). Determination of sufficiency values of canopy reflectance vegetation indices for maximum growth and yield of cucumber. *European Journal of Agronomy*, *84*, 1–15. https://doi.org/10.1016/j.eja.2016.12.008

Pandit, S., Tsuyuki, S., & Dube, T. (2018). Estimating above-ground biomass in subtropical buffer zone community forests, Nepal, using Sentinel 2 data. *Remote Sensing*, *10*(4), 601. https://doi.org/10.3390/rs10040601

Pearson, R. L., & Miller, L. D. (1972). *Remote mapping of standing crop biomass for estimation of the productivity of the short-grass prairie*. In Proceedings of the 8th International Symposium on Remote Sensing of Environment (pp. 1357–1381). Environmental Research Institute of Michigan.

Poudel, A., Shrestha, H. L., Mahat, N., Sharma, G., Aryal, S., Kalakheti, R., & Lamsal, B. (2023). Modeling and mapping of aboveground biomass and carbon stock using Sentinel-2 imagery in Chure region, Nepal. *International Journal of Forestry Research*, *2023*, 5553957. https://doi.org/10.1155/2023/5553957

Ravindranath, N. H., & Ostwald, M. (2008). Remote sensing and GIS techniques for terrestrial carbon inventory. In *Carbon inventory methods: Handbook for greenhouse gas inventory, carbon mitigation and round wood production projects* (pp. 181–199). Springer. https://doi.org/10.1007/978-1-4020-6547-7_14

Roujean, J. L., & Breon, F. M. (1995). Estimating PAR absorbed by vegetation from bidirectional reflectance measurements. *Remote Sensing of Environment*, *51*(3), 375–384. https://doi.org/10.1016/0034-4257(94)00114-3

Rouse, J. W., Jr., Haas, R. H., Schell, J. A., & Deering, D. W. (1974). *Monitoring vegetation systems in the Great Plains with ERTS*. In *Third ERTS-1 Symposium* (Vol. 1, Sect. A). NASA, Goddard Space Flight Centre.